ELSEVIER

Journal of Power Sources 54 (1995) 103–108

JOURNAL OF POWER SOURCES

The $Li_{1+x}Mn_2O_4$/C system Materials and electrochemical aspects

J.M. Tarascon [a], F. Coowar [a], G. Amatuci [a], F.K. Shokoohi [a], D.G. Guyomard [b]

[a] *Bellcore, Red Bank, NJ 07701, USA*

[b] *IMN, Université de Nantes, France*

Abstract

The importance of the synthesis conditions of $Li_{1+x}Mn_2O_4$ on its electrochemical performance, namely, capacity fading and initial capacity is discussed. By using a well-defined thermal treatment and a particular nominal composition, $x=0.05$, one can overcome the problem of capacity fading that was previously experienced with $LiMn_2O_4$ while, at the same time, enhancing the usable capacity. The importance of the thermal treatment in terms of oxygen stoichiometry effects and how cyclic voltammetry can be used to optimize $Li_{1+x}Mn_2O_4$ powders have been discussed.

Keywords: Rechargeable lithium batteries; Lithium; Manganese dioxide; Lithium-ion cells

1. Introduction

AA-size, Li-ion rechargeable battery prototypes based on $Li_{1+x}Mn_2O_4$/C were recently constructed [1,2] with capacity, power rate, and cycle life similar to that obtained for the same size $LiCoO_2$/C cells [3]. However, Li-ion cells based on $LiMn_2O_4$ electrodes offer several advantages over the Li-ion cells based on Ni [4] or Co oxides. These include: (i) a lower electrode cost resulting from natural abundance and lower cost of Mn compared to Co or Ni, and (ii) lower toxicity and established recycling methods for Mn-based oxide materials. Thus, on the basis of its economy and environmental acceptability, this system is more desirable for volume manufacturing. One concern, however, has been the lack of electrolytes that are resistant to oxidation at voltages greater than 4.2 V, i.e., the voltage at which the Li intercalation/de-intercalation process takes place in $LiMn_2O_4$. We recently reported an EC–DMC-based electrolyte composition [5] that is compatible with $LiMn_2O_4$ electrodes and is resistant to oxidation up to 4.8 V at 25 °C. $LiMn_2O_4$/EC + DMC + $LiPF_6$/C test cells were efficiently cycled more than 2000 times at 25 °C and 500 times at 55 °C between 2 and 4.5 V [6]. Thus, one of the main obstacles to a wider use of the spinel $LiMn_2O_4$ in Li-ion cells, namely, the lack of suitable electrolytes, has been eliminated.

Another important problem standing in the way of the wider use of the spinel as a positive electrode has been the capacity fading of $LiMn_2O_4$/electrolyte/Li cells during cycling. Electrolyte oxidation was proposed as the cause of this phenomenon. However, the persistence of capacity fading in cells that contained an electrolyte resistant to oxidation up to 5 V led us to search for alternative sources of this problem. $LiMn_2O_4$ belongs to the family of spinels whose structure can be described with the general formula $[A]_{Te}[B_2]_{Oc}O_4$ where the A and B metal cations are located in the tetrahedral and octahedral sites, respectively. However, this structure is complicated by the possibility of cation mixing which, if complete, could result in a compound of the general formula $[B]_{Te}[AB]_{Oc}O_4$ called inverse spinel. It is well documented that within the spinel family, the degree of cation mixing is strongly dependent on the thermal history of the sample. In addition, previous reports [7] have shown that the physical properties, e.g., magnetic or optical, of the spinel compounds are extremely sensitive to their synthesis conditions. Thus, it was important to determine whether or not the Li intercalation/de-intercalation process within $LiMn_2O_4$ was sensitive to heat treatment. We embarked on an extensive study of the thermal synthesis of lithiated manganese oxides containing a varying Li content, and on the effect of synthesis conditions on the electrochemical properties of the resulting materials. The effect of

SSDI 0378-7753(94)02048-8

substituting small amounts of 3d-metals (Fe, Co) for Mn in $LiMn_2O_4$ on the capacity fading phenomena was also investigated. We have found that the electrochemical performance of $LiMn_2O_4$ powders (for example, the capacity fading upon cycling) depends strongly on the sample treatment, namely, on the sample annealing/cooling rate, rather than on the nature or morphology of the Li- or Mn-based precursors.

2. Experimental

$Li_xMn_2O_4$ samples in the powder form were obtained by mixing stoichiometric amounts of Li salts (x) and Mn-based oxides. The precursor materials were Li_2CO_3 and electrochemical manganese dioxide (EMD-MnO_2) (IBA #15 was used as received) unless specified otherwise. The samples were heated to 800 °C in air, maintained at this temperature for about 48 h, cooled to room temperature and ground in a ball mill. This heat treatment sequence was repeated again, and the samples were then re-annealed to 800 °C, kept at this temperature for 24 h, and cooled to room temperature either by quenching (cooling time = 2 min; samples denoted Q), or by slow cooling (cooling at a rate of 3 to 5 °C/h from 800 to 500 °C and 50 °C/h from 500 °C to room temperature; samples denoted SC).

3. Results

The resulting $Li_xMn_2O_4$ samples in the powder form were investigated by X-ray powder diffraction technique. The material is a single-phase for lithium contents ranging from 0.95 to 1.15. Within this range of Li solubility, for the slowly cooled samples the spinel a-axis decreases from 8.25 to 8.21 Å with an increase in Li content, x. Beyond this range of solubility the system is multi-phase with Mn_2O_3 and Li_2MnO_3 as the main impurity phases for x lower than 0.95 and greater than 1.15, respectively. A decrease in the cooling rate from the same annealing temperature for a sample having a well-defined composition also resulted in a decrease in the cubic a-axis parameter (Fig. 1). Quenched samples exhibit larger values of the a-axis parameter than slowly cooled samples and are multi-phase when quenched from temperatures greater than 850 °C. For instance, the X-ray powder diffractogram of a $LiMn_2O_4$ sample quenched from 1100 °C reveals only broad Bragg peaks located at the 2θ positions expected for the orthorhombic $LiMnO_2$ phase.

As a way to understand the origin of the changes in lattice parameters between SC and Q samples, we performed thermogravimetric analysis (TGA) in air on some of the $LiMn_2O_4$ specimens. No weight change was observed up to 750 °C (Fig. 2). However, the TGA

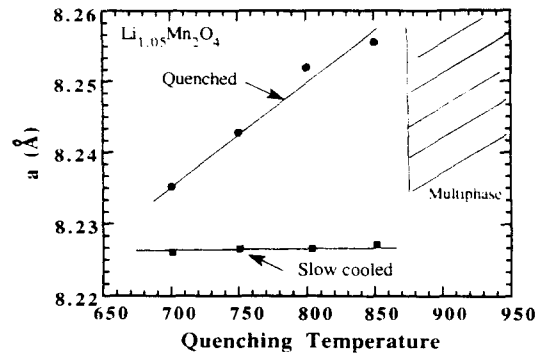

Fig. 1. Variation of the cubic a-lattice parameter for the spinel $Li_{1+x}Mn_2O_4$ as a function of the cooling rate from various annealing temperatures.

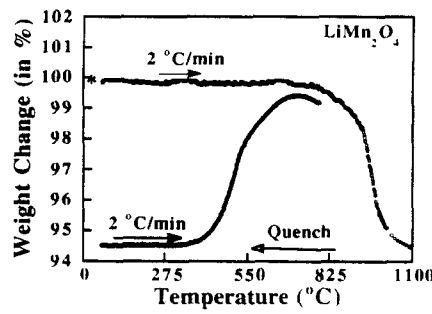

Fig. 2. TGA traces for a $Li_{1+x}Mn_2O_4$ specimen heated in air to 1100 °C, quenched and re-heated.

trace deviates from constant value at higher temperatures; a weight loss as large as 5.5% at an annealing temperature of 1100 °C was observed. This change in weight is reversible, as indicated by the 5% weight uptake of a sample that has been quenched from 1100 °C and re-annealed in air at a rate of 2 °C/min.

This reversible weight change corresponds to a loss of oxygen from the spinel phase $LiMn_2O_{(4\pm\Delta x)}$ with oxygen being respectively released or uptaken upon heating or cooling of $LiMn_2O_4$. Among the most likely possibilities to account for the observed oxygen loss are the loss of oxygen from the spinel structure or through a reversible phase decomposition. The spinel structure consists of a cubic closed-packed lattice of oxygen atoms, a type of arrangement that does not favor oxygen vacancies. TGA data have shown reversible changes in oxygen content as high as 5% by weight. This corresponds to a change in x of 0.5. Although a small fraction of oxygen vacancies could exist within the spinel structure, this fact itself cannot account for the observed value of 0.5 per unit formula. Thus, oxygen release through phase decomposition must occur to explain the observed TGA data.

Among the most likely phase decomposition reactions are:

$$2LiMn_2O_4 \longrightarrow 2LiMnO_2 + Mn_2O_3 + 0.5O_2$$
$$\text{(oxygen loss} = 4.4\%) \qquad (1)$$

$$3LiMn_2O_4 \longrightarrow 3LiMnO_2 + Mn_3O_4 + O_2$$
$$\text{(oxygen loss} = 5.9\%) \qquad (2)$$

Both these reactions are consistent with the observation that samples quenched from 1100 °C contain $LiMnO_2$ as the main impurity phase, but the absence of other well-defined extra Bragg peaks prevents any attempt to distinguish between reactions (1) and (2). However, based on the magnitude of the weight changes observed, reaction (2) seems the most likely candidate.

The importance of the synthesis conditions, namely cooling rate and annealing temperature, on the change in oxygen content, Δx, in $LiMn_2O_{(4\pm\Delta x)}$ is illustrated in Figs. 3(a) and (b). Note that the oxygen loss, Δx, increases with an increase in the annealing temperature or with an increase in the cooling rate when starting from the same annealing temperature.

In order to maintain the charge balance in $LiMn_2O_4$, changes in oxygen stoichiometry must be associated with changes in the oxidation state of Mn. The reduction of Mn^{4+} to Mn^{3+} at higher temperature could result in a structural instability of the spinel structure at high temperatures. We investigated the high temperature phase diagram of $LiMn_2O_4$ by annealing $LiMn_2O_4$ powders at various temperatures ranging from 800 to 1000 °C in steps of 10 °C, followed by quenching to preserve their deficiency in oxygen. We found [8] that the $LiMn_2O_4$ spinel evolves from a cubic to tetragonal symmetry with an increase in the quenching temperature (Fig. 4). The range of temperatures at which the tetragonal spinel phase can be obtained is very narrow (895–910 °C). For $T > 910$ °C the removal of oxygen occurs through a phase-decomposition reaction as indicated by the coexistence of the tetragonal spinel and orthorhombic $LiMnO_2$ phase. In short, upon heating of $LiMn_2O_4$ in air, the following mechanism is believed to occur.

(i) oxygen loss from $LiMn_2O_4$ occurs with the formation of oxygen vacancies even if cation vacancies already exist;

(ii) the decomposition of the cubic spinel to the tetragonal '$LiMn_2O_{3.8}$' phase takes place with the formation of a biphasic mixture to produce;

(iii) pure tetragonal '$LiMn_2O_{3.8}$'-phase, and

(iv) the decomposition of the tetragonal phase to $LiMnO_2$ + other products finally takes place as suggested by reaction (2).

The whole sequence is a reversible, kinetically slow process that depends on the particle sizes, that have to react to re-form $LiMn_2O_4$. Notations indicating cationic vacancies within the spinel were purposely omitted from the above formula for reasons of simplicity.

Potentiostatic studies have been carried out to determine how the changes in oxygen stoichiometry affect the electrochemical properties of these materials. Swagelok test cells with a Li–metal negative electrode and 1 M $LiPF_6$/EC–DMC electrolyte allowed us to carry

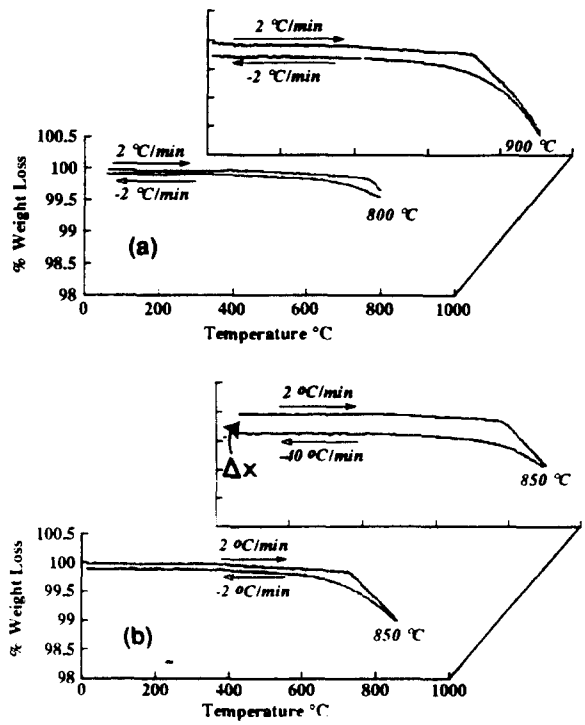

Fig. 3. TGA traces for (a) $Li_{1+x}Mn_2O_4$ samples annealed to 800 °C and 900 °C and cooled at 2 °C/min. (b) TGA traces for the same samples annealed at 850 °C and cooled either at 2 °C/min or 40 °C/min.

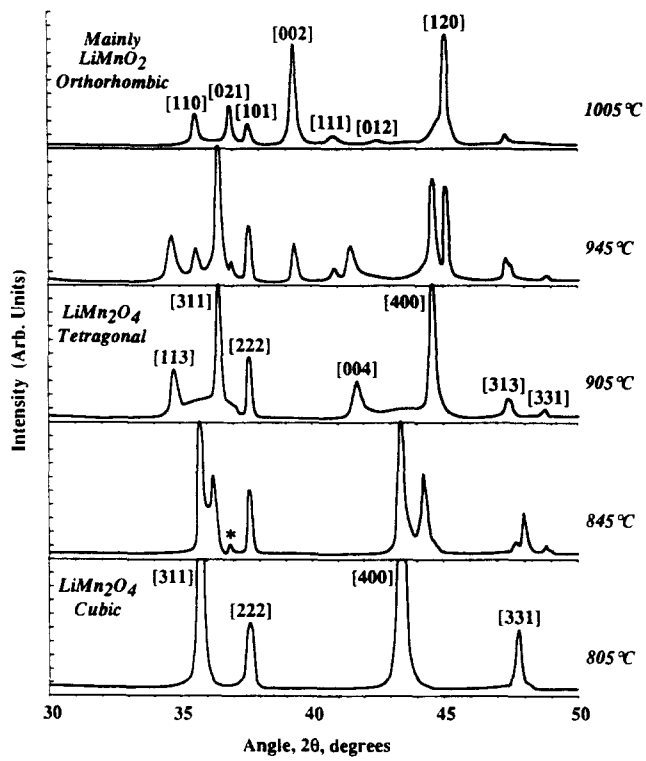

Fig. 4. Powder X-ray diffraction patterns illustrating the cubic to tetragonal phase transition in $LiMn_2O_4$.

out studies of the Li intercalation process in $LiMn_2O_4$ up to 5 V versus Li with negligible electrolyte oxidation. Besides the two well-known peaks at 4.1 and 4.2 V, representing the Li intercalation/de-intercalation processes in the spinel $LiMn_2O_4$, these studies revealed two fully reversible, additional peaks at approximately 4.5 and 4.9 V versus Li, that correspond to Li intercalation/de-intercalation processes in the spinel $LiMn_2O_4$. The magnitude of these small peaks is extremely sensitive to the synthesis conditions of $LiMn_2O_4$. For the same quenching sequence (Fig. 5(a)), the magnitude of the 4.5 V peak decreases with an increase in the lithium content. A decrease in the 4.5 V peak (Fig. 5(b)) is also observed with a decrease in the cooling rate, e.g., in going from Q to SC. The replacement of Mn by Co or Fe (not shown) also resulted in the disappearance of the 4.5 V peak.

We studied the cycling performance of $LiMn_2O_4$/electrolyte/Li Swagelok cells using $Li_{1+x}Mn_2O_4$ powders of various nominal compositions and annealing sequences as a positive electrode. The measurements were carried out using constant-current cyclers with a $\pm 1\%$ current stability. The wide range of results (Fig. 6(a)) indicates the strong influence of both the annealing sequence and the nominal composition on the electrochemical properties of $LiMn_2O_4$. From this plot we extract the curves that correspond to capacity fading for the Q (either cubic or tetragonal) and SC samples (Fig. 6(b)). The capacity fading for the quenched samples was initially larger than that for the slowly cooled

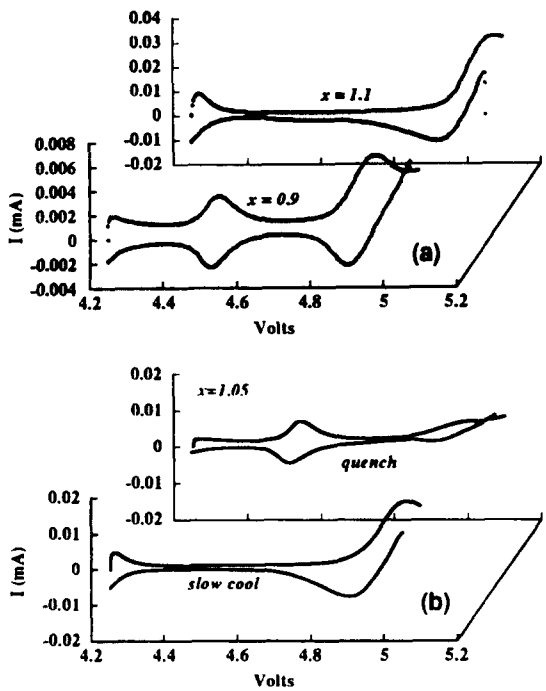

Fig. 5. Cyclic voltammograms within the 4.2–5.1 V potential range for $Li_xMn_2O_4$/electrolyte/Li cells. The effect of nominal compositions, x, (a) in $Li_xMn_2O_4$ and (b) cooling rate on the amplitude of the 4.5 and 4.9 V peaks, respectively, is shown.

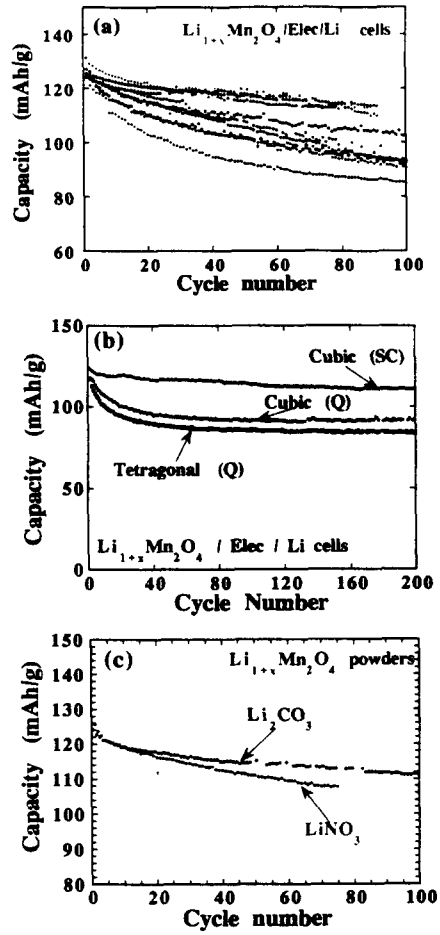

Fig. 6. Variation of the capacity as a function of the cycle number for Swagelok cells with $Li_{1+x}Mn_2O_4$ made by: (a) changing the annealing sequence and composition; (b) fixing the nominal Li compositions to 0.5 and by changing the cooling sequence, and (c) mixing EMD-MnO_2 with either $LiNO_3$ or Li_2CO_3. The samples were either slowly cooled (SC), quenched (Q), or fast-cooled.

samples. However, after the first fifty cycles, both the slowly cooled and the quenched samples showed a similar capacity fading. The capacity fading for the tetragonal spinel phase was similar to that of the quenched cubic phase. This data clearly indicates that slowly cooled $LiMn_2O_4$ samples exhibit optimum electrochemical performance. For a 10% Co-substituted sample, the decay in capacity during cycling was similar to that of a non-substituted, slowly cooled $LiMn_2O_4$ sample with a lower initial capacity. The importance of the nominal composition, x, in $Li_xMn_2O_4$ on the initial capacity was also studied. The samples with x greater than 1 showed the largest capacity with a maximum at 125 mAh/g for the sample of nominal composition $Li_{1.05}Mn_2O_4$ ($x = 0.05$).

The best $Li_{1+x}Mn_2O_4$ powders for battery applications are made by slow cooling of a mixture with the nominal composition '$Li_{1.05}Mn_2O_4$'. These powders are characterized by a cubic lattice parameter always smaller than 8.23 Å, and by the absence of the 4.5 V peak.

Consequently, the two additional intercalation peaks observed in the cyclic voltammogram of the spinel can directly be used as fingerprints of electrochemically optimized $Li_{1+x}Mn_2O_4$ powders. As discussed elsewhere [8], cation mixing within the spinel, is at the origin of these peaks.

In an attempt to understand the origin of the difference in capacity fading between cells containing $LiMn_2O_4$ synthesized under various conditions, the cells shown in Fig. 6(a) were opened after the cycling test, and both the positive and the negative electrodes were characterized by X-ray and energy dispersive spectroscopy (EDS). An important finding was the presence of Mn at the negative electrode, as shown in Fig. 7. There are two possibilities to account for this observation, one being that some $LiMn_2O_4$ particles moved to the negative electrode by electrophoresis and the other, that some Mn ions went into solution and were reduced to Mn metal at the negative electrode. If electrophoresis were taking place, the amount of Mn determined at the negative should strongly depend on the particle size which was not the case. The amount of Mn plated at the negative electrode, as determined by EDS, was plotted as a function of the capacity fading of the corresponding cells. In spite of the relatively large scatter in the experimental data, we consistently found that the samples showing the largest capacity fading were also those having the largest amount of Mn plated at the lithium electrode. The amount of Mn deposited at the negative electrode was independent, within the accuracy of the measurement, of the particle size of the $Li_{1+x}Mn_2O_4$ powders.

Having determined the optimum synthesis conditions for the electrochemically optimized $Li_xMn_2O_4$ powders, we studied the effects of the nature and morphology of the precursors on the electrochemical properties of the resulting powders. For instance, $LiNO_3$ was used

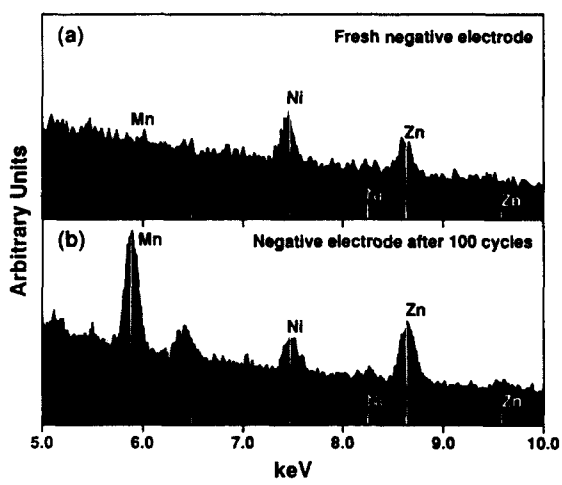

Fig. 7. Energy dispersive spectroscopy (EDS) for (a) fresh Li electrodes, and (b) for Li electrodes from $Li_{1+x}Mn_2O_4$/electrolyte/Li cells that have been cycled 100 times.

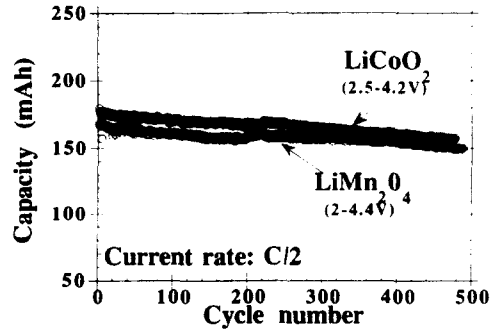

Fig. 8. The capacity fading for two Li-ion cells using either $LiMn_2O_4$ or $LiCoO_2$ as the positive electrode, and coke as the negative electrode.

instead of Li_2CO_3 and β-MnO_2 or Mn acetates were used instead of EMD-MnO_2 to prepare $Li_{1+x}Mn_2O_4$ powders. The samples were prepared using the thermal regime that was previously identified to produce the highest quality $LiMn_2O_4$ powders. The use of $LiNO_3$ instead of Li_2CO_3 as a Li precursor result in $Li_{1+x}Mn_2O_4$ powders that have a larger surface area (4 m^2/g for powders made from $LiNO_3$ or 0.8 m^2/g for powders made from Li_2CO_3). However, the electrochemical performance of the resulting material in terms of capacity fading is identical (Fig. 8). Bearing in mind that it is the surface area of the positive electrode composite that controls the rate of electrolyte oxidation, having electrodes with large surface area may not always be desirable, especially if good high-temperature performance is required.

4. Conclusions

The importance of the synthesis conditions of $Li_{1+x}Mn_2O_4$ powders on their electrochemical performance has been discussed. By using a well-defined thermal treatment and a particular Li content ($x = 0.05$), one can overcome the problem of capacity fading that has been previously experienced with $LiMn_2O_4$. An electrochemically optimized $Li_{1.05}Mn_2O_4$ powder was used to construct Li-ion laboratory test cells which exhibited very low capacity fading during battery cycling (Fig. 8). The synthesis of $LiMn_2O_4$ is less forgiving than the synthesis of $LiCoO_2$, but when the optimum conditions are followed, Li-ion cells based on either $LiCoO_2$ or $LiMn_2O_4$ cells show similar capacity fading, as indicated in Fig. 8. Because of cost and environmental considerations, we expect $LiMn_2O_4$ to become the material of choice for tomorrow's Li-ion technology. However, the three oxide candidates for this technology have a capacity limited to 0.5 Li per 3d-metal atom. Consequently, the capacity of Li-ion cells is only 66% of that of similar size Ni–metal hydride cells. To improve the capacity of Li-ion cells, more effort should be

directed to the search for new electrode materials, either positive or negative, with improved capacity.

Reversible capacities as high as 400 mAh/g ($Li_{1.1}C_6$) and 600 mAh/g ($Li_{1.6}C_6$) have recently being reported [9] for both the natural and synthetic graphites. Increasing the capacity of the graphite negative electrode is important. However, we should note that most of the recently reported highly graphitized carbons with specific densities around 600 mAh/g are disordered, low density materials. Thus, in terms of applications, having a carbon with a capacity of 600 mAh/g but with a low packing density might not present a significant advantage over a carbon with a smaller specific capacity, but with higher packing density. In addition, these high specific capacity graphites intercalate Li at potentials that are close to that of Li metal. One could then ask the question whether by playing this game we are not defeating the original purpose of enhancing the safety of a Li-ion cell. The real challenge should be to search for the negative electrode materials that would intercalate Li at higher voltages than graphite while maintaining its specific capacity both at comparable cost and availability.

Simple calculations indicate that if one doubles the specific capacity of the positive electrode, e.g., by using an oxide that could reversibly intercalate 1 Li instead of 0.5 Li per 3d-metal, one could increase the specific capacity of the cell by 68%. In contrast, if one doubles the specific capacity of the negative electrode ($LiC_6 \rightarrow Li_2C_6$), one increases the overall specific capacity of the cell by only 12%. Thus, to improve the performance of the Li-ion technology, namely in terms of specific capacity, we believe that the main effort should be directed towards the synthesis of new positive-electrode materials, i.e., various lithiated oxides that could reversibly intercalate one Li atom per 3d-metal atom at about 4 v versus Li. The potential impact of such an effort is well worth the risk.

Acknowledgements

The authors would like to thank A. Gozdz, R. McKinnon, R. Rousset and F. Thaillades for useful discussions.

References

[1] J.M. Tarascon and D. Guyomard, *Electrochim. Acta, 38* (1993) 1221.
[2] J.M. Tarascon, D. Guyomard and G.L. Baker, *J. Power Sources, 43/44* (1993) 689.
[3] T. Nagaura and K. Tazawa, *Prog. Batteries Solar Cells, 9* (1990) 20.
[4] J.R. Dahn, U. Von Sacken, M.R. Jukow and H. Al-Janaby, *J. Electrochem. Soc., 137* (1991) 2207.
[5] D. Guyomard and J.M. Tarascon, *US Patent No. 5192629* (1993).
[6] D. Guyomard and J.M. Tarascon, *J. Electrochem. Soc., 140* (1993) 3071.
[7] J.L. Baudour, F. Bouree, M.A. Fremy, R. Legros, A. Rousset and B. Gillot, *Physica B, 180/181* (1992) 97.
[8] J.M. Tarascon, W.R. McKinnon, F. Coowar, T.N. Bowner, G. Amatucci and D. Guyomard, *J. Electrochem. Soc., 141* (1994) 1421.
[9] K. Sato, M. Noguchi, A. Demachi, N. Oki and M. Endo, *Science, 264* (1994) 556.